

General Disclaimer

One or more of the Following Statements may affect this Document

- This document has been reproduced from the best copy furnished by the organizational source. It is being released in the interest of making available as much information as possible.
- This document may contain data, which exceeds the sheet parameters. It was furnished in this condition by the organizational source and is the best copy available.
- This document may contain tone-on-tone or color graphs, charts and/or pictures, which have been reproduced in black and white.
- This document is paginated as submitted by the original source.
- Portions of this document are not fully legible due to the historical nature of some of the material. However, it is the best reproduction available from the original submission.

**NASA TECHNICAL
MEMORANDUM**

NASA TM X-74004

NASA TM X-74004

(NASA-TM-X-74004) APPLICATION OF A MODIFIED
COMPLEMENTARY FILTERING TECHNIQUE FOR
INCREASED AIRCRAFT CONTROL SYSTEM FREQUENCY
BANDWIDTH IN HIGH VIBRATION ENVIRONMENT

N77-17103

(NASI) 21 p EC A02/MF A01

Unclass

CSC1 01D G3/08

15613

**APPLICATION OF A MODIFIED COMPLEMENTARY FILTERING
TECHNIQUE FOR INCREASED AIRCRAFT CONTROL
SYSTEM FREQUENCY BANDWIDTH IN HIGH VIBRATION
ENVIRONMENT**

BY

JOHN F. GARREN, JR., FRANK R. NIESSEN,
TERENCE S. ABBOTT, AND KENNETH R. YENNI

JANUARY 1977

This informal documentation medium is used to provide accelerated or special release of technical information to selected users. The contents may not meet NASA formal editing and publication standards, may be revised, or may be incorporated in another publication.



National Aeronautics and
Space Administration

Langley Research Center
Hampton, Virginia 23665



*For sale by the National Technical Information Service
Springfield, Virginia 22161

NATIONAL AERONAUTICS AND SPACE ADMINISTRATION

APPLICATION OF A MODIFIED COMPLEMENTARY FILTERING TECHNIQUE FOR
INCREASED AIRCRAFT CONTROL SYSTEM FREQUENCY BANDWIDTH IN
HIGH VIBRATION ENVIRONMENT

by John F. Garren, Jr., Frank R. Niessen, Terence S. Abbott,
and Kenneth R. Yenni

Langley Research Center

SUMMARY

Advanced control techniques for aircraft rely on the use of high-gain feedback from motion sensors to achieve improved performance in terms of disturbance rejection and response compliance. In high vibratory environments such as helicopters experience, however, excessive noise amplification occurs even for modest gain levels, precluding to a great extent the benefits of high-gain systems. In the present study, a modified complementary filtering technique for estimating aircraft roll rate was developed and flown in a research helicopter to determine whether higher gains could be achieved. The results indicated that use of this technique did, in fact, permit a substantial increase in system frequency bandwidth because, in comparison with first-order filtering, it reduced both noise amplification and control limit-cycle tendencies.

INTRODUCTION

Advanced control techniques for aircraft rely on the use of high-gain feedback from motion sensors to achieve improved performance in terms of disturbance rejection and response compliance. A direct measure of the degree of success that can be realized in achieving these benefits is the closed-loop frequency bandwidth, which is a function of maximum feedback gain that can be achieved. In practice, feedback gain level is limited by either noise amplification or control limit cycle, or by a combination of both.

In high vibratory environments such as helicopters experience, excessive noise amplification occurs even for modest gain levels. The noise encountered in helicopters is associated primarily with rotor-induced vibration and, therefore, contains harmonics of the rotational frequency. The frequency content corresponding to one cycle per rotor revolution and to n cycles per revolution, where n represents the number of blades per rotor, is usually the most bothersome from a control feedback standpoint because the amplitude is large and the frequency is so low that the control actuators and control

surface aerodynamics can respond. Attempts to eliminate this low-frequency noise by classical filtering techniques introduce significant lag, which aggravates the limit-cycle problem, thereby requiring reduction in the feedback gain level. For feedback control applications where low gains can provide acceptable performance, such as in stability augmentation systems, classical filtering techniques are usually adequate. For the implementation of model-following and other control concepts requiring achievement of high-gain feedback, however, the situation has been less than satisfactory, with a severe operating compromise among noise, limit cycle, and performance.

In the present study, a modified complementary filtering technique for estimating roll rate was developed and tested using a highly instrumented research helicopter at the Langley Research Center. The modified technique was similar to conventional complementary filtering techniques in that a signal having the desired properties was generated by combining the low-frequency content of a signal from one source with the high-frequency content of a signal from a different source. It differed, however, in that only one of the sources was a motion sensor; the other signal was generated by a simple model which predicted the helicopter response on the basis of the command to the electronic flight control system. The purpose of the study was to determine whether such a technique would permit the use of higher feedback gain levels and thereby provide increased closed-loop frequency bandwidth, which was deemed essential for planned research applications of this helicopter. During development of the complementary filter, effects of variations in filter time constant and in mismatch between the plant and the filter model were explored. Also, a comparison was made of the relative effectiveness of classical filtering versus complementary filtering for achieving stable closed-loop performance in conjunction with high gains. Results are presented in terms of time histories of the commanded and actual roll rates.

SYMBOLS AND DEFINITIONS

s	-	Laplacian operator
G_1	-	gain of acceleration lead term from desired-response model to ECS
G_2	-	rate-error-signal gain, sec^{-1}
G_3	-	attitude-error-signal gain, sec^{-2}
G_4	-	gain of unstable damping loop used to cancel inherent damping of helicopter, sec^{-1}
L_δ	-	control sensitivity in desired-response model, $\text{rad/sec}^2/\text{cm}$
L_p	-	angular acceleration proportional to and opposing roll rate, sec^{-1}

- ζ - damping ratio
 τ - filter time constant, sec
 $\hat{\phi}$ - aircraft estimated roll rate when the complementary filter was used, or low-passed roll rate when first-order filter was used, rad/sec
 $\dot{\phi}_C$ - calculated roll rate based on signal to electronic control system and used as input to high-pass portion of complementary filter, rad/sec
 $\dot{\phi}_E$ - actual roll-rate error; defined as $(\dot{\phi}_M - \dot{\phi}_H)$, rad/sec
 $\hat{\dot{\phi}}_E$ - estimated roll-rate error; defined as $(\dot{\phi}_M - \hat{\phi})$, rad/sec
 ϕ_H - aircraft roll attitude sensed by vertical gyro, rad
 $\dot{\phi}_H$ - aircraft roll rate sensed by rate gyro, rad/sec
 ϕ_M - aircraft roll attitude commanded by desired-response model dynamics, rad
 $\dot{\phi}_M$ - aircraft roll rate commanded by desired-response model dynamics, rad/sec
 $\ddot{\phi}_M$ - aircraft roll acceleration commanded by desired-response model dynamics, rad/sec²
 ω_n - undamped natural frequency, rad/sec

COMPLEMENTARY FILTER DESIGN

General

A simplified block diagram of the model-following control system for which the complementary filter was developed and in which it was evaluated is shown in figure 1. Although a similar system implementation was also employed for the pitch and yaw degrees of freedom, systematic variations in the system design parameters were explored for only the roll degree of freedom. As a further aid to understanding the system and the ensuing discussion, the analog computer diagram, which was used for synthesis of the electronic portion of the system, is presented in figure 2.

The model-following control concept has been used for many years as a research tool for in-flight simulation, and its principles, if not already, will probably be applied eventually to stabilization system and autopilot design. Briefly, the model-following concept is based on the principle of forming error signals between the response commanded by a desired set of model dynamics and the response measured by a set of motion sensors. These error signals, in turn, are used to drive the aircraft control surfaces in order to null the error and, thus, achieve response compliance.

The only significant difference between the model-following system shown in figure 1 and the concept used during the handling qualities research investigation reported in reference 1 was the incorporation of the complementary filter to provide an estimate of angular rate for forming the rate-error closure. Removal of the signal path consisting of the "simplified plant model" and the "high-pass filter" elements in figure 1 reverts the complementary filter to a classical first-order filter, which corresponds to the filtering scheme frequently used in helicopter stabilization systems. Individual elements of the model-following system employed in this investigation are discussed in the following sections.

Desired-Response Model

The desired-response shaping was achieved by a second-order model which generated acceleration, rate, and attitude commands corresponding to pilot stick control inputs. The model parameters were selected to provide an attitude sensitivity (i.e., attitude change per unit pilot control input) of 0.04 rad/cm, a damping ratio of 0.76, and an undamped natural frequency of 1.4 rad/sec.

Sensors

Both the rate gyro and the vertical gyro were standard flight quality instruments. They were mounted directly to the airframe without any type of shock mounting. In an attempt to minimize pickup of local structural vibrations, the rate gyro was attached to a metal plate that was floor-mounted to the aircraft's primary structure. The dimensions of the metal plate, on which other equipment was also mounted, were 120 by 216 by 0.95 cm. The vertical gyro was mounted on the shelf of a well-braced instrumentation table.

Electronic Control System (ECS)

The ECS is discussed more fully in the "Description of Equipment" section of the paper. For purposes of this section, the function of the ECS was to convert electrical signals from the analog computer into proportional displacement of the aircraft control surfaces. The ECS was, of course, a modification that was made to the CH-47 when it was converted for use as a research helicopter.

Complementary Filter

The term "complementary filter," as used in this paper, includes the elements shown in the block so labeled in figure 1.

Theoretical considerations.- Ideally, the function of the complementary filter was to derive a noise-free, lag-free estimate of the aircraft angular rate. The filter attempted to do this by passing only the low-frequency content of the rate gyro output, $\dot{\phi}_H$, and summing it with only the high-frequency content of the rate, $\dot{\phi}_C$, calculated by the simplified plant model. The time constant, τ , for both portions of the filter must be identical in order to satisfy the requirement that the net effect yield an uncontaminated rate output. That this is true may be demonstrated as follows: Using the rule for summing transfer functions that are in parallel, the transfer function, $F(s)$, that represents the combined effect of the high-pass and low-pass portions of the complementary filter becomes:

$$F(s) = \underbrace{\frac{\tau_1 s}{\tau_1 s + 1}}_{\text{high-pass}} + \underbrace{\frac{1}{\tau_2 s + 1}}_{\text{low-pass}}$$

If $\tau_1 = \tau_2$, the above equation becomes:

$$F(s) = \frac{\tau_1 s + 1}{\tau_1 s + 1} = 1$$

Hence, for this condition of identical values for τ , the filter acts as a unity transfer function insofar as the basic signal is concerned and contributes no dynamics to the system.

Practical considerations.- The success of the approach depended on being able to find a single value of τ which was both large enough to reject noise on the gyro signal and yet small enough to reject, or washout, long-term errors in the calculated rate. Experience with classical filters in helicopters had shown that filter time constants which were large enough to attenuate noise adequately introduced so much phase lag that additional gain still could not be achieved without reducing system stability and exciting limit cycle. The typical compromise between noise and limit cycle usually resulted in selection of a time constant on the order of 0.05 sec. The basic question, then, appeared to be whether a time constant for the complementary filter existed that would be sufficiently large to eliminate noise amplification and yet sufficiently small to mask the effects of simplifying assumptions used in the generation of $\dot{\phi}_C$; and, finally, whether use of the complementary filter would, in fact, avoid the limit-cycle problems encountered using classical filtering.

Simplified plant model.- Because of complexities in the actual plant dynamics, to do more than grossly approximate the plant within the complementary filter would be impractical. Initially in this investigation, it was assumed that the plant could be modeled as a first-order response, i.e., that a steady moment acting on the helicopter would result in a steady-state roll rate. The parameters for this model were obtained from available stability derivative data for the CH-47 helicopter presented in reference 2. Later, variations in the plant model were explored, with the level of the plant damping parameter first being increased to approximately twice the value of the corresponding CH-47 parameter, and then being reduced to zero. The later case, wherein potentiometer A was set at zero (corresponding to an acceleration model), required minor modifications to the computer diagram shown in figure 2 in order to avoid saturation of integrator A. With the modification in circuitry, $\dot{\phi}_C$ was no longer generated as a recordable parameter, since its identity was lost in combining the functions of integrators A and B.

Error Closures and Gains

Four signals were summed and the resultant signal was used to drive the ECS. One of the four signals was a lead term based on angular acceleration commanded by the model. The gain, G_1 , for the lead term was set to give the correct initial response based on knowledge of the CH-47 angular acceleration per unit control. The signal having gain G_4 was an unstable rate feedback, the purpose of which was to enable a corresponding increase of the rate-error gain with no additional increase in noise or limit cycle. The gain, G_4 , was selected to provide cancellation of the CH-47 roll-rate damping, which was approximately 0.6 sec^{-1} . For systems where only low gains had been achievable, this refinement had been proven to be of significant value. The two remaining signals were error closures; one was a rate-error closure and the other was an attitude-error closure.

Rate-error closure.- The rate-error signal was based on the estimated rate error, which was generated as the difference in the model roll rate, $\dot{\phi}_M$, and the estimated roll rate, $\hat{\phi}$, generated by the complementary filter. The rate-error gain, G_2 , is usually adjusted experimentally in flight to attain the maximum level that can be tolerated from the standpoint of control system noise or limit cycle; the higher the level of G_2 , the better the closed-loop system performance.

Attitude-error closure.- The attitude-error signal, ϕ_E , was generated as the difference in the model roll attitude, ϕ_M , and the roll attitude, ϕ_H , measured by the vertical gyro. From past experience, it was believed that this signal would be relatively noise free and that filtering would not be warranted. The gain, G_3 , for the attitude-error closure was based strictly

on dynamics considerations: Note, for instance, that G_3 is equivalent to the spring constant in a second-order system and, hence, equal to ω_n^2 , while G_2 is equivalent to damping and, hence, equal to $2\zeta\omega_n$. Summarizing:

$$G_2 = 2\zeta\omega_n$$

$$G_3 = \omega_n^2$$

Manipulating these equations yields:

$$G_3 = \frac{[G_2]^2}{4\zeta^2}$$

Once the value of G_2 has been established as described above, the value of G_3 can be determined readily for any desired value of damping ratio. A value of $\zeta = 0.7$ was maintained in these tests.

DESCRIPTION OF EQUIPMENT

Test Aircraft

The test aircraft, a CH-47B helicopter shown in figure 3, was provided by the U.S. Army in support of the Langley Research Center VALT (VTOL Approach and Landing Technology) Program. An extensive listing of the stability characteristics of the CH-47B is presented in reference 2, along with a tabulation of the aircraft's physical characteristics. The aircraft was extensively modified and instrumented to support the VALT Program, but only the systems and modifications pertinent to this investigation are described herein. A signal flow diagram for the VALT CH-47 research control system is shown in figure 4.

Pilot controls located on the right-hand side of the cockpit were converted to a fly-by-wire system by disconnecting their mechanical linkages from the basic control system and installing control position transducers, which transmitted electrical signals proportional to control displacement. Other special features of the system included the electronic control system (ECS), the clutch transfer mechanism (CTM), hardover monitoring equipment (HOME), and provision for stability augmentation system (SAS) canceling.

ECS. - The ECS electronics performed several functions. It contained the logic and relays involved in arming and engaging/disengaging the research control system. Also, prior to system engagement, it canceled ECS input

signals to prevent engage transients. And, finally, it permitted selection of the SAS-canceling function which enabled the SAS to be fully functional at all times for safety purposes, yet preventing the SAS from effecting the research results in any significant manner.

The ECS actuator had 100-percent authority but, for safety considerations, was rate limited to permit a maximum control system velocity of 16.5 cm/sec as measured at the safety pilot's lateral control-stick grip.

CTM.- The clutch transfer mechanism provided a mechanical disconnect between the research system and the basic control system when the ECS was not engaged. Prior to engagement, the ECS side of the clutch (the input side) was driven by the ECS to synchronize its position with the output side of the clutch in order to insure full authority capability. The output side of the clutch was mechanically connected to the standard control linkage so that the safety pilot's control was backdriven by the ECS commands. The CTM slip level was adjusted so that the safety pilot could overpower the ECS, should he so desire, by applying an opposing force to his control.

HOME.- The function of the hardover monitoring system was to disengage the ECS when it detected hardover failures. The detection threshold was set at about 80 percent of the maximum ECS actuator rate. The HOME was a digital system having triplex redundancy and built-in self-test capability. It performed failure detection in the roll channel by sampling the ECS actuator position at a rate of 11.8 Hz and deriving actuator velocity based on the amount of displacement since the previous sample.

Recording Instrumentation

A Langley-developed PADS (piloted aircraft data system) provided sensor signal conditioning and recording on magnetic tape. As configured for this study, the system provided a data recording capability for 75 channels of continuous data and 22 discrete channels. Of the continuous data channels, 5 were high-frequency VCO (voltage controlled oscillator) channels; the remaining 70 were PCM (pulse code modulation). The VCO channels were used exclusively to record the more critical parameters involved in this investigation, including $\dot{\phi}_M$, $\dot{\phi}_H$, and $\dot{\phi}$. The PCM channels, which provided a resolution of approximately 0.4 percent of full scale, were used to record all of the motion sensors and control position transducers; and the discrete channels, to indicate events such as ECS engagement. Also, a time code, generated by the PADS, was recorded on the tape.

TEST PROCEDURES

Although systematic variations in the test parameters were made for only the roll degree of freedom, the model-following concept, using complementary filters, was also employed during the tests for the pitch and yaw degrees.

of freedom. For control of the vertical degree of freedom, the fly-by-wire collective control (on the right-hand side of the cockpit) was electrically coupled to the mechanical collective control (on the left-hand side of the cockpit) to provide a one-to-one motion relationship between the two.

The typical test run involved hover maneuvers, including precision hover over a spot, hover turns, lateral translation, and quick starts and stops. Some conditions were also tested to a speed of 110 knots. The reason for not exploring higher speeds was that the HOME had not been sufficiently qualified. The tests were conducted with both the SAS and the SAS-canceling systems operating, providing, in effect, a SAS off condition.

RESULTS AND DISCUSSION

Comparison of Complementary and First-Order Filtering

The effects of the complementary filtering technique on closed-loop system behavior are compared with those of classical first-order filtering in figure 5. The figure presents time histories of roll rate as commanded by the model and as accomplished by the helicopter. Also included are time histories of the filter output which, for the complementary filter cases, represents the estimated rate. During these tests, the rate-error gain, G_2 , was set at 4.0 sec^{-1} , while the attitude-error gain, G_3 , was set at 8.0 sec^{-2} , providing a damping ratio of approximately 0.7 for the combination. (Initially it had been planned to obtain the comparison at $G_2 = 6.0 \text{ sec}^{-1}$, but the control system motion was so violent at this gain for the first-order filter that data could not be obtained; the HOME repeatedly interpreted the noise as a hardover failure and immediately disengaged the system.) For these runs, the plant model used in the complementary filter computation was a first-order-response representation.

In reviewing the time histories in figure 5, the actual rate, $\dot{\phi}_H$, should be examined in comparison with the commanded rate, $\dot{\phi}_M$. Observing, for example, the first-order filter case corresponding to the smallest time constant, $\tau = 0.05 \text{ sec}$, it is apparent from the similarity between the two traces that model-following performance was quite good. Assume, however, that the control system was excessively noisy, which it was, and that the filter time constant was increased to reduce the noise. With an increase to $\tau = 0.10 \text{ sec}$, it is seen that the helicopter rate no longer followed the model very precisely, but had a tightly damped oscillatory characteristic with a period of about 1.0 Hz. (The high-frequency control system noise was observed, of course, to decrease.) As the first-order filter time constant was further increased to 0.20 sec and, finally, to 0.50 sec, the low-frequency oscillation became progressively more violent, with the helicopter exhibiting no tendency whatsoever to follow the model.

The lower portion of figure 5 shows the corresponding behavior of the system with the complementary filter. Note that for neither $\tau = 0.50$ sec nor even for $\tau = 1.0$ sec were there any apparent tendencies toward system instability. In fact the safety pilot, whose control levers were backdriven by the electronic control system which permitted him to directly observe the effects of parameter variations on control system motion, reported that there was no degradation detectable for either of these complementary filter cases and that the system was extremely smooth. Note, also, that for even these extremely large time constant values, the model-following performance was reasonably good.

Effect of Plant Model Assumptions Used in Complementary Filter Computation

The purpose of this phase of the tests was to determine sensitivity of model-following performance to intentional mismatch between the dynamics of the CH-47 helicopter and the plant dynamics used by the complementary filter in deriving the high-frequency content of the estimated roll rate. For these tests, the error-signal gains were $G_2 = 6.0 \text{ sec}^{-1}$ and $G_3 = 18.0 \text{ sec}^{-2}$, providing a damping ratio of approximately 0.7 for the combination. The results are shown in figure 6, where, for three assumed levels of damping, one may compare the model-following performance achieved. The comparison is most readily made by observing the time history of the rate-error signal, $\dot{\phi}_E$, which is the difference in the model rate, $\dot{\phi}_M$, and the measured rate, $\dot{\phi}_H$.

The data are grouped in a four-by-three matrix, where each column represents a fixed filter time constant and each row represents one of the three plant models. The top row shows time histories obtained with the damping level of the plant model set at zero, thereby providing a simple acceleration representation of the plant. The second row, with $L_p = 0.56 \text{ sec}^{-1}$, corresponded to the best approximation to the actual plant, and the third row, with $L_p = 1.0 \text{ sec}^{-1}$, to a damping that was nominally twice the CH-47 damping. Sensitivity to plant model assumptions would be expected to become more pronounced as the filter time constant was increased since, the larger the time constant, the more heavily the computed rate is weighted in deriving the estimated rate. Conversely, the shorter the time constant, the more heavily the measured rate is weighted. This effect is apparent in the upper row of data of figure 6, where it may be seen that the estimated rate, $\hat{\phi}$, looks very much like the actual rate, $\dot{\phi}_H$, for $\tau = 0.05$ sec, but differs greatly for $\tau = 1.0$ sec. As a worst case situation for examining the sensitivity to plant model assumptions, therefore, a long time constant should be considered. Accordingly, for a value of $\tau = 1.0$ sec (column four of the figure), data were obtained for each of the three damping levels. Interestingly, even for such an unrealistically large time constant, the model-following performance was

reasonably good for all cases, even though the estimated rate, particularly for the $L_p = 0$ case, appears to be considerably unlike the actual rate.

It is evident from these results that the model-following performance was not sensitive to mismatch between the actual plant and the plant model used in the complementary filter computation. It seems reasonable to conclude that good model-following performance was maintained, even though the estimated rate indicated serious defects, because the attitude-error signal was operating at a very high gain, G_3 . Nevertheless, the credit ultimately belongs to the complementary filter, for without it, damping ratio considerations would have prohibited attainment of large values for G_3 .

Even though using an acceleration model to represent the plant dynamics simplified the system implementation somewhat and provided satisfactory model-following performance, some words of caution are in order at this point. For this special case, it can be shown that the system frequency bandwidth is attenuated at low frequencies by the factor $\frac{1}{1 + G_2\tau}$. In other words, representing the effective rate and attitude-error signal gains as G_2' and G_3' , respectively:

$$G_2' \Big|_{s \rightarrow 0} = G_2 \left(\frac{1}{1 + G_2\tau} \right)$$

$$G_3' \Big|_{s \rightarrow 0} = G_3 \left(\frac{1}{1 + G_2\tau} \right)$$

It is clear from these equations that the larger the value of τ , the smaller the static gain of the system. If the plant experiences large trim changes or has other low-frequency characteristics which must be thoroughly masked, the loss of effective gain at low frequencies may be too great a price to pay for the extra simplicity afforded by using an acceleration model. When the rate representation of the plant is used, there is no loss of low-frequency gain, i.e., $G_2' \Big|_{s=0} = G_2$ and $G_3' \Big|_{s=0} = G_3$.

Benefits of Complementary Filtering

Although the benefits attributable to the complementary filtering technique would be directly related to the particular application and would be a function of the severity of the vibratory environment, it is perhaps instructive to examine the improvement realized in the present application. In the case of the VALT CH-47, the maximum gains while retaining satisfactorily smooth behavior of the control system were $G_2 = 3.0 \text{ sec}^{-1}$ and $G_3 = 4.5 \text{ sec}^{-2}$

for the first-order filter ($\tau = 0.05$ sec). By way of comparison, for the complementary filter ($\tau = 0.2$ sec), even smoother control system behavior was achieved with $G_2 = 6.0 \text{ sec}^{-1}$ and $G_3 = 18.0 \text{ sec}^{-2}$. As a conservative estimate of the benefit, then, the complementary filter permitted doubling the rate-error gain and permitted multiplication of the attitude-error gain by a factor of 4.

With respect to the selection of a value for the time constant for the complementary filter, the smallest value that will reduce noise amplification to a satisfactory level should be used. One reason for this is that simplifying assumptions about the plant model are more valid for smaller time constants. In the case of this application in the VALT CH-47, the best value would probably be between 0.1 and 0.2 sec, when the rate-error gain, G_2 , is set at 6.0 sec^{-1} . At the lower time constant, the "one per rev" noise was still somewhat apparent, but it appeared to be totally eliminated at the higher value.

CONCLUSIONS

A flight investigation was conducted with a research helicopter to determine the effectiveness of a complementary filtering technique for estimating aircraft angular rate for use in high-gain control feedback applications where a high vibratory environment exists. The complementary filtering technique was evaluated in the context of providing the rate-error closure for a high-gain model-following control system. The following conclusions were drawn:

1. Use of the complementary filtering technique permitted substantial increase in system frequency bandwidth due to simultaneous reduction in noise amplification and control limit-cycle tendency as compared with results obtained when using a conventional first-order filter.
2. Overall system performance was insensitive to mismatch between the dynamics of the plant and the plant model used in the complementary filter computation; for filter time constant values as large as 1.0, satisfactory model-following performance was achieved even though only a very simple plant model was used.
3. Although excellent model-following performance was obtainable for a relatively broad range of values for the test parameters using the complementary filtering technique, the filter time constant selected should be no larger than required to achieve a satisfactorily low noise level.
4. The achievement of higher rate-error gains, as made possible by the complementary filtering technique, made permissible the use of higher attitude-error gains.

REFERENCES

1. Niessen, Frank R.; Kelly, James R.; Garren, John F., Jr.; Yenni, Kenneth R.; and Person, Lee H.: The Effect of Variations in Controls and Displays on Helicopter Instrument Approach Capability. NASA TN D-8385, January 1977.
2. Ostroff, Aaron J.; Downing, David R.; and Rood, William J.: A Technique Using a Nonlinear Helicopter Model for Determining Trims and Derivatives. NASA TN D-8159, May 1976.

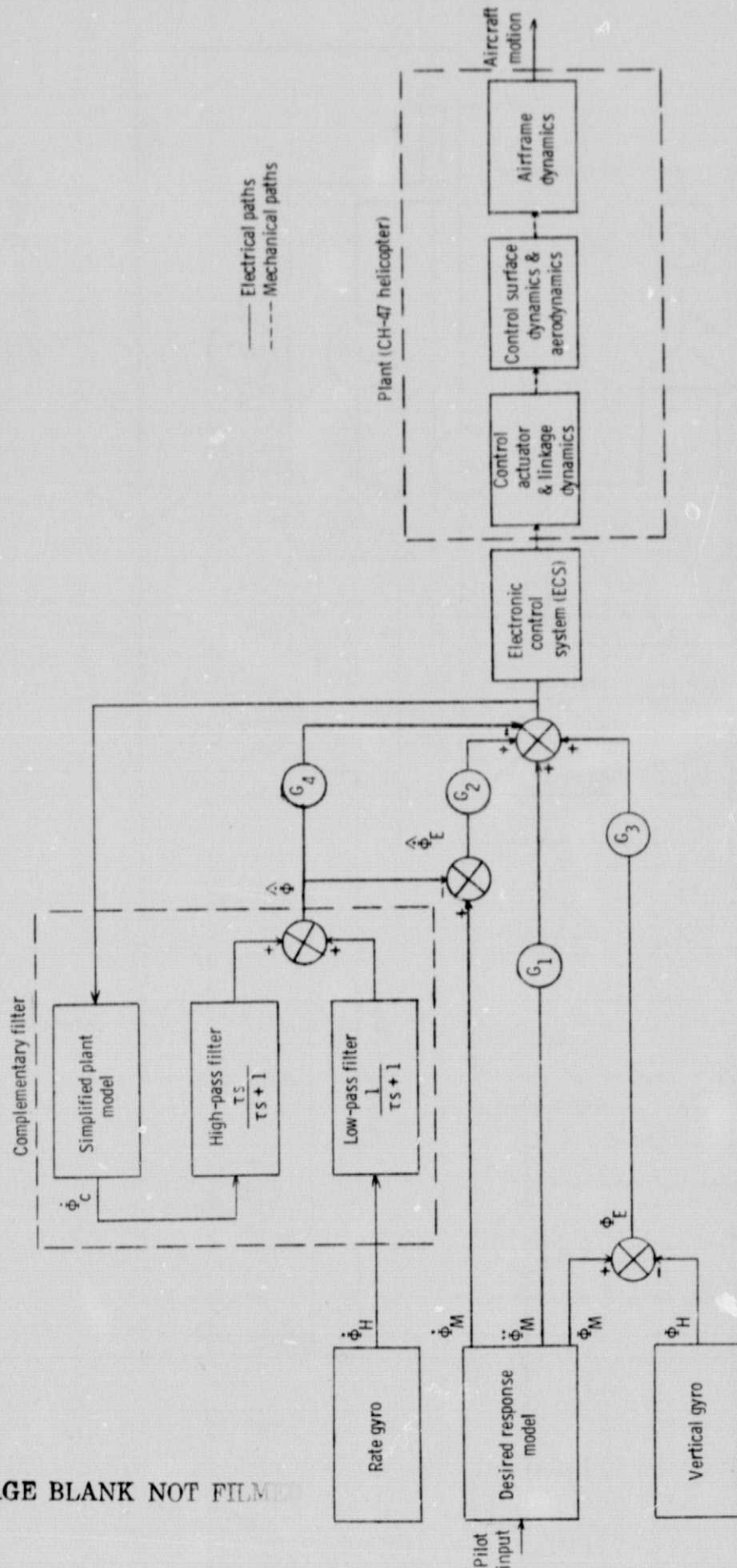


Figure 1. - Schematic diagram of model-following control system employing complementary filter.

PROCEEDING PAGE BLANK NOT FILM

ORIGINAL PAGE IS
OF POOR QUALITY

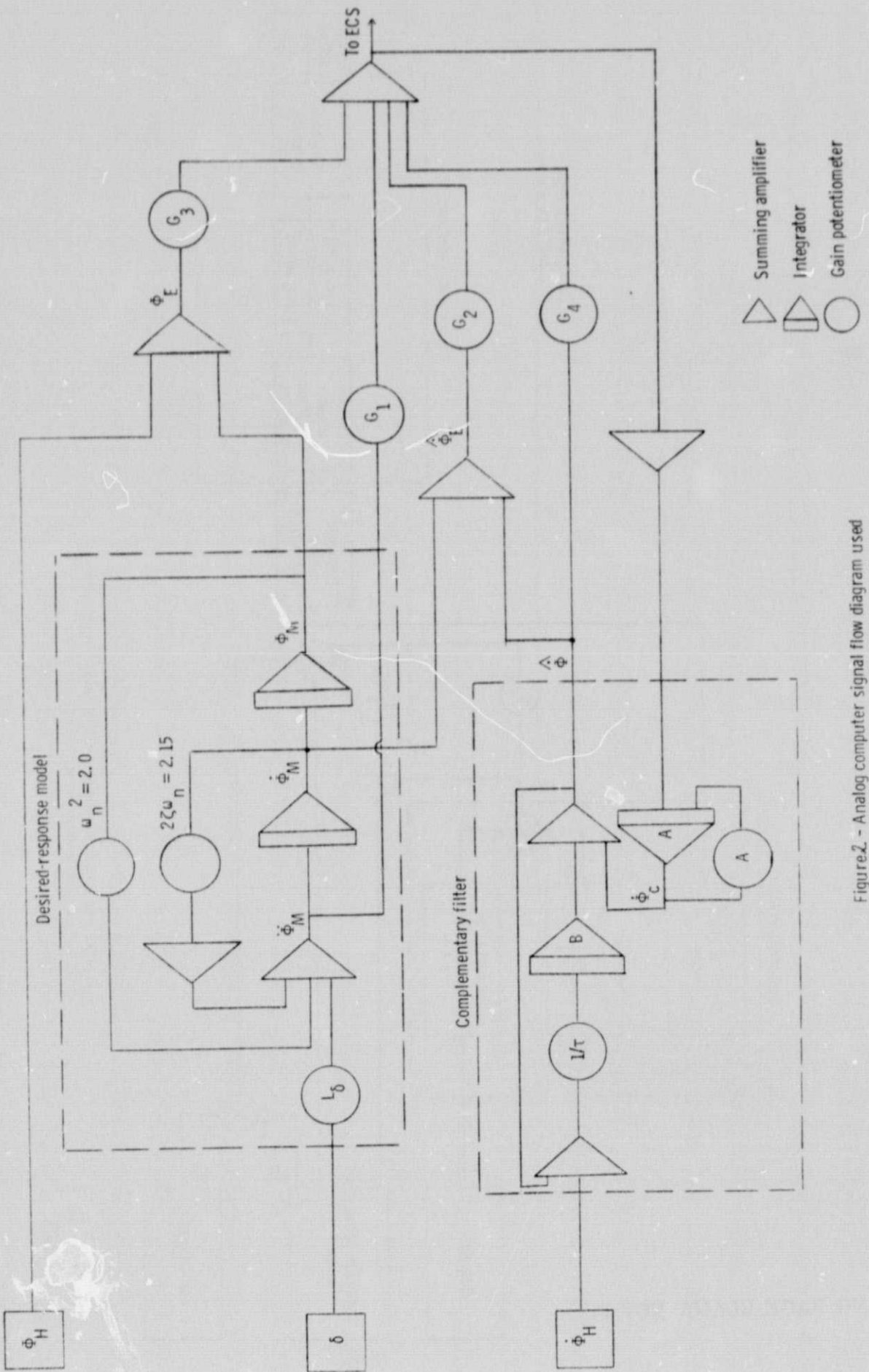


Figure 2 - Analog computer signal flow diagram used for synthesis of model following system employing complementary filter.

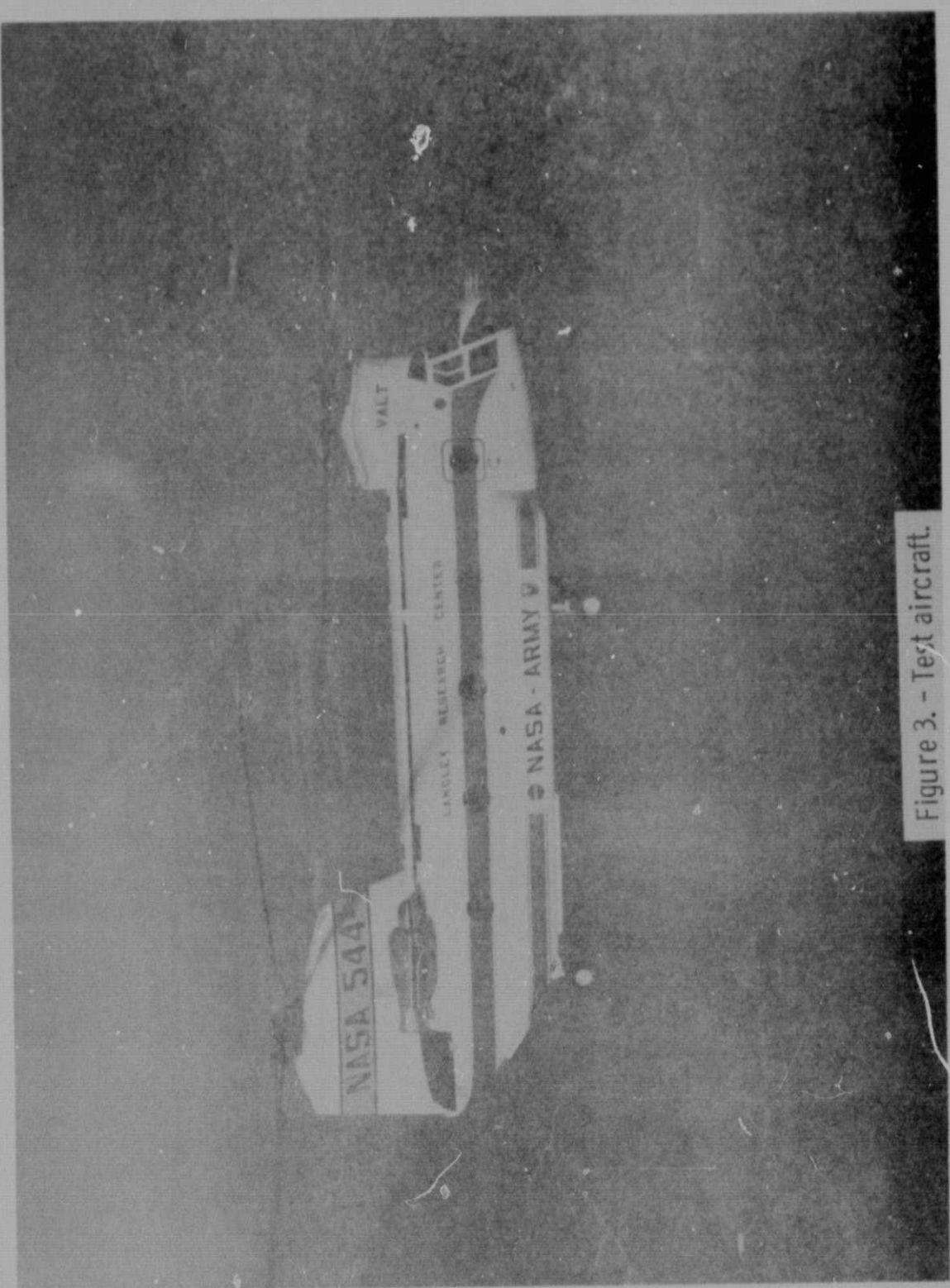


Figure 3. - Test aircraft.

ORIGINAL PAGE IS
OF POOR QUALITY

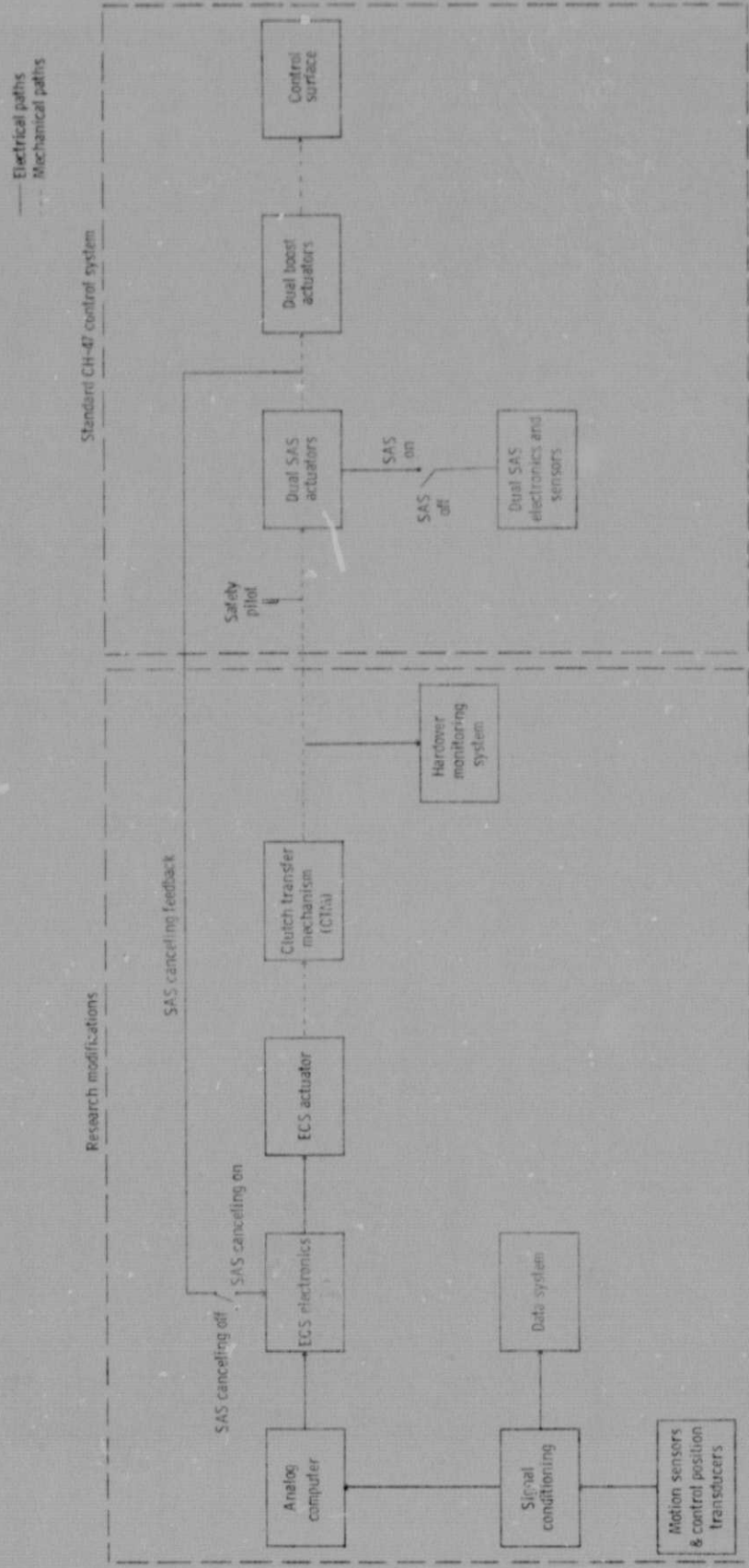
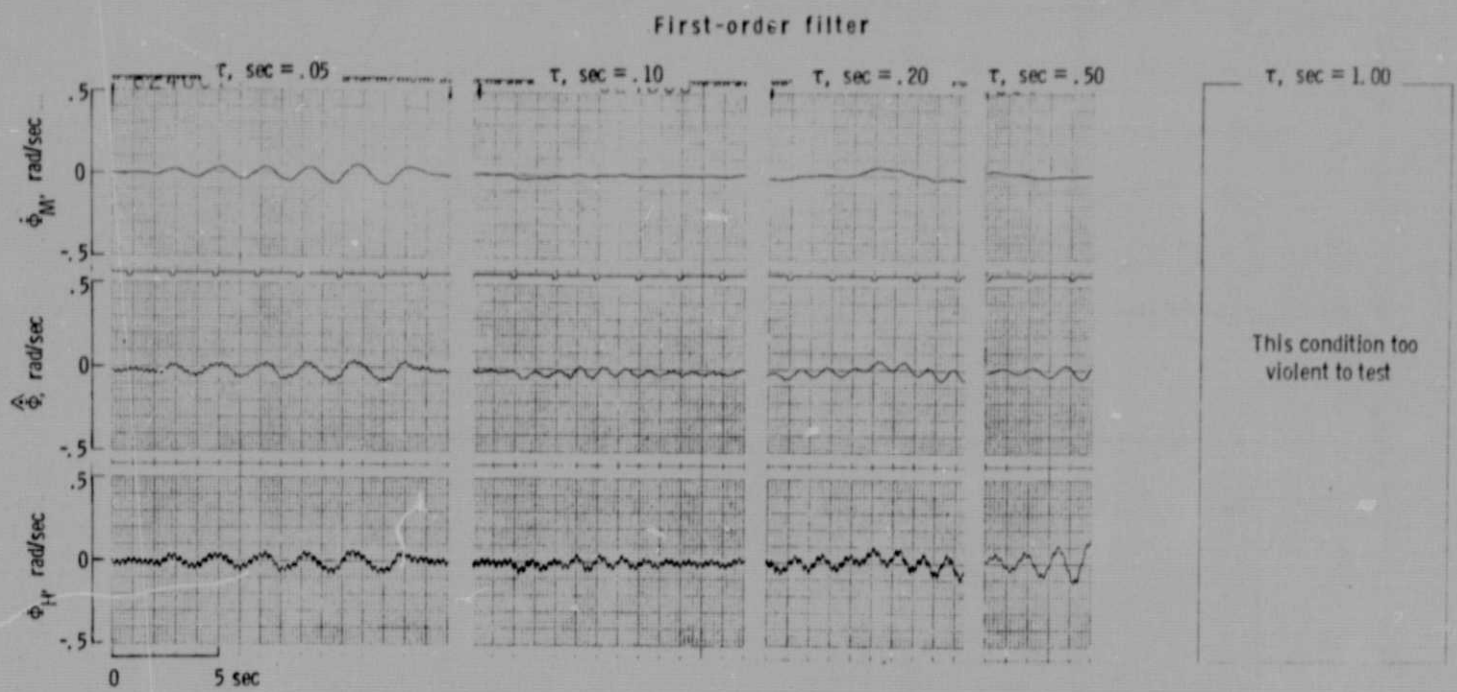


Figure 4 - Vert CH-47 control system flow diagram
(typical axis).

ORIGINAL PAGE IS
OF POOR QUALITY



Complementary filter

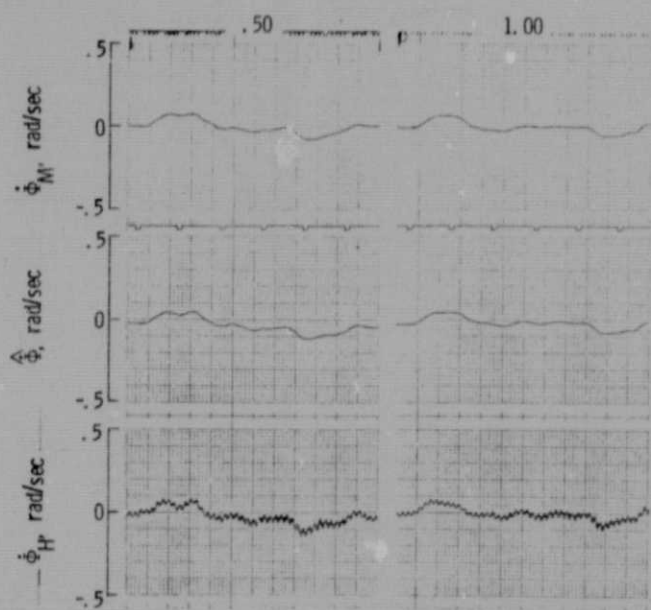


Figure 5. - Effect of filter time constant on closed-loop stability
 $(G_2 = 4.0 \text{ sec}^{-1})$.

ORIGINAL PAGE IS
OF POOR QUALITY

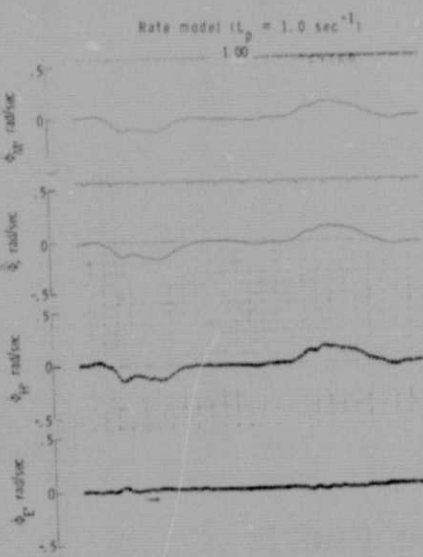
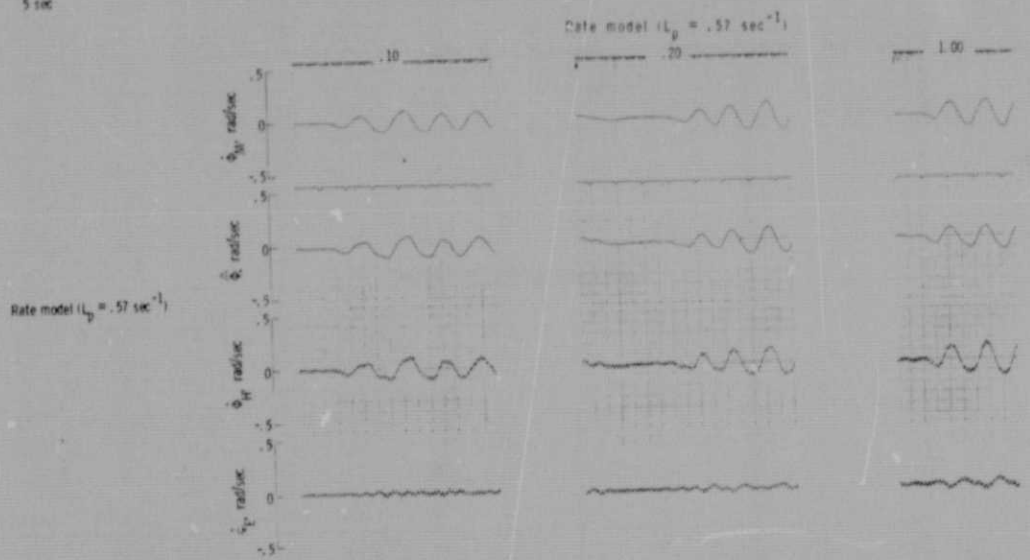
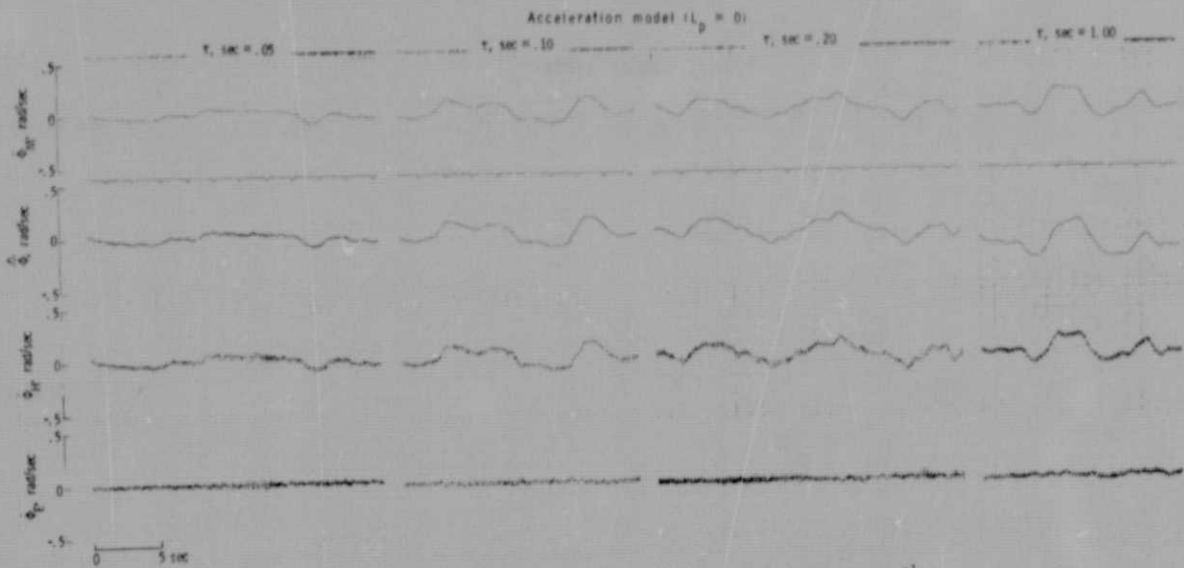


Figure 6. - Effect of model dynamics used in complementary filter computation.
 $(G_2 = 6.0 \text{ sec}^{-1})$